Three-dimensional forest stand height map production utilizing airborne laser scanning dense point clouds and precise quality evaluation

Umut G Sefercik [1],
Ayhan Atesoglu [2]

In remote sensing, estimation of the forest stand height is an ever-challenging issue due to the difficulties encountered during the acquisition of data under forest canopies. Stereo optical imaging offers high spatial and spectral resolution; however, the optical correlation is lower in dense forests than in open areas due to an insufficient number of matching points. Therefore, in most cases height information may be missing or faulty. With their long wavelengths of 0.2 to 1.3 m, P-band and L-band synthetic aperture radars are capable of penetrating forest canopies, but their low spatial resolutions restrict the use of single-tree based forest applications. In this study, airborne laser scanning was used as an effective remote sensing technique to produce large-scale maps of forest stand height. This technique produces very high-resolution point clouds and has a high penetration capability that allows for the detection of multiple echoes per laser pulse. A study area with a forest coverage of approximately 60% was selected in Houston, USA, and a three-dimensional color-coded map of forest stands was produced using a normalized digital surface model technique. Rather than being limited to the number of ground control points, the accuracy of the produced map was assessed with a model-to-model approach using terrestrial laser scanning. In the accuracy assessment, the standard deviation was used as the main accuracy indicator in addition to the root mean square error and normalized median absolute deviation. The absolute geo-location accuracy of the generated map was found to be better than 1 cm horizontally and approximately 40 cm in height. Furthermore, the effects of bias and relative standard deviations were determined. The problems encountered during the production of the map, as well as recommended solutions, are also discussed in this paper.

Keywords: Airborne Laser Scanning, Forest Stand Height Map, First Echo, Last Echo, NDSM

Introduction

Over the past few decades, remote sensing techniques that provide three-dimensional (3D) geo-information have become indispensable, particularly for land-related research that analyzes the Earth's surface. Forest modeling is an area that requires repetitive and costly terrestrial measurements for the creation of an inventory based on single tree-related parameters, such as tree species and their distribution, timber volume and the mean tree height (Koch et al. 2006). Today, information on

most of these parameters is obtained by generating 3D height models with remotely sensed data. However, the accuracy of these models remains an open question. This study was partially designed to provide an answer to this question by producing high resolution (25 cm) 3D maps of forest stand height using an effective remote sensing method, namely airborne laser scanning (ALS), and validating the produced map through model-to-model visual and statistical methods. The term 3D height model involves three forms of the

main triangular irregular network: a digital surface model (DSM), a digital elevation model (DEM) and a digital terrain model (DTM). In the field of forestry, the DSM demonstrates the canopy of forest at the look-angle of the remote sensing instrument, which includes the X and Y planimetric coordinates and the altitude, Z. DEMs and DTMs also represent bare earth underlying the terrain of forest. Information obtained from a DEM and a DTM are very similar, with the only difference that the DTM provides additional information from hard and soft break-lines and mass points measured with triangular irregular networks.

In flat and open areas, the 3D earth modeling potential of remote-sensing techniques is comparable to that of terrestrial measurements; however, remotely sensed data may be distorted in inclined or forest-covered topographies, due to imaging geometries and limited sensing capabilities. 3D earth modeling that uses passive remote-sensing data derived from space-borne stereo optical imaging and photogrammetry is an operator-dependent semi-automatic process. Even if digital images have very high spatial and spectral resolution, the performance of area-based automatic

□ (1) Department of Geomatics Engineering, Bulent Ecevit University, 67100 Zonguldak (Turkey); (2) Department of Forest Engineering, Faculty of Forestry, Bartin University, 74100 Bartin (Turkey)

@ Umut G Sefercik (sefercik@beun.edu.tr)
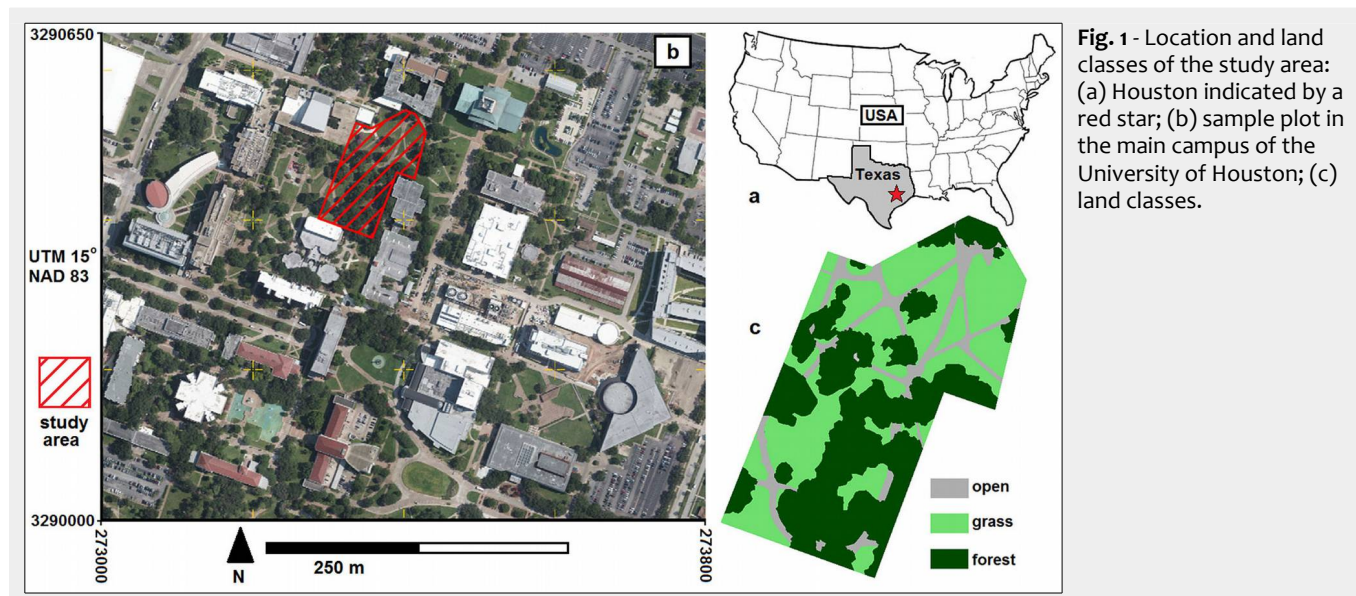
Fig. 1 - Location and land classes of the study area: (a) Houston indicated by a red star; (b) sample plot in the main campus of the University of Houston; (c) land classes.

image-matching algorithms is limited and the operator must visually assign additional matching points to stereo images to improve the accuracy of the final products. Moreover, in dense forest areas, due to low optical correlation, the functionality of the operator becomes even more significant, and due to the lack of details (such as information on constructions, break-lines and fire ways), the operators can only identify a limited number of matching points. Despite the availability of image enhancement methods based on band combinations, such as false color and the normalized difference vegetation index, they are not sufficient to improve the accuracy of the final 3D product to a satisfactory level. On the other hand, synthetic aperture radar (SAR) imagery offers a fully automatic process for generating DSMs and has the advantage of utilizing interferometric synthetic aperture radar (InSAR) technology. However, the long-wavelength penetrative bands (P and L) of SAR do not meet the spatial resolution required for studies of single-tree based forest inventory. The remaining SAR imaging bands (such as S, C and X) fail to penetrate forest canopies and obtain accurate and sufficient information about the underlying bare topography. Due to these limitations, ALS has grad-

ually become the primary technique for mapping forest areas, which offers rapid and highly accurate 3D topographic point clouds that have traditionally not been provided by competing remote sensing technologies (Baltsavias 1999, Hill et al. 2000). With its forest penetration capability, achieved through the detection of multiple echoes per laser pulse and dense point clouds, ALS is considered by the scientific community as an effective solution for generating DEMs (Lohr 1998, McIntosh et al. 2000, Shan & Sampath 2005, Mandlburger et al. 2007, Baligh et al. 2008, Liu 2008, Akay et al. 2012).

In this study, a 3D map of forest stand height was created in a forest-covered area located on the main campus of the University of Houston, which utilized a normalized digital surface model (nDSM) *alias* canopy height model technique. The nDSM is a differential model of the generated DSM and DTM, and it is one of the most reliable and frequently used techniques employed to estimate forest stand heights (Sterenczak et al. 2008, Smreček 2012). Unlike many studies published in the literature, we identified the most crucial and error-prone points in nDSM generation using dense ALS point clouds, and offer suggestions of how to obtain an accurate model. More-

over, rather than using ground control points (GCP), the accuracy of the generated map was controlled using a model-to-model approach based on the reference nDSM obtained from the terrestrial laser scanning (TLS) data.

This paper is organized as follows: first, the study area and materials are described followed by the methodology section, which gives details about the production of a 3D forest stand height map and accuracy assessment. Later, the generated 3D map and the results of geo-location accuracy assessment are presented, followed by the conclusion.

Materials and methods

Study area and materials

Considering the requirements of this analysis, a forest-covered area located in the main campus of the University of Houston in Texas, USA was chosen as the study area. The study area is 13,000 m², and it is comprised of three different land classes: open, grass and forest. The orthometric height of the area ranges from 10 to 33 m. Fig. 1 presents the location and land classes of the study area.

The ALS flights used in this study were completed by the National Center for Airborne Laser Mapping (NCALM) based at the University of Houston. During the flights, the entire area of the main campus (3 × 9 km = 27 km²) was covered and an Optech Gemini airborne laser terrain mapper was used to collect very high-resolution (VHR) point clouds. Due to the intensity of the point clouds, and considering the capability of the computers and software used, the data was divided into 27 tiles of size 1 × 1 km. The TLS measurements were obtained with a Riegl VZ-400® instrument (RIEGL Laser Measurement Systems GmbH, Horn, Austria). The characteristics of the instruments and measurements are listed in Tab. 1.

As shown in Tab. 1, the ALS and TLS data

Tab. 1 - Characteristics of used instruments and measurements.

Parameter	ALS	TLS
Instrument	Optech Gemini ALTM	Riegl VZ-400
Date	23/06/12	13/11/13
Point density (m²)	45	≈10000 points ≤ 10m horizontal distance
Pulse rate (kHz)	167	300
Wavelength (nm)	1064	1550
Scan frequency (Hz)	0-70	n/a
Beam divergence (mrad)	0.25	0.35
Field of view (°)	-25 to +25	360 horizontal/-40 to +60 vertical
Flight altitude (m)	1000	n/a
Number of returns	4	~Unlimited

were not collected during the same period of the year. However, since the trees in the study area are primarily live oaks, they maintain foliage all year. Therefore, there was no need to collect leaf-on and leaf-off data, and except for some minor differences due to vegetation, we did not expect to see a significant difference between the ALS and TLS data. This was confirmed by visual inspection of the point clouds, which indicated only minimal and smaller changes than observed in the nDSM assessment.

Methodology description

The production of a 3D map of forest stand height, and the assessment of its accuracy, were performed in five main stages, as presented in Fig. 2. Prior to the procedure, NCALM completed the post-processing and calibration of the collected ALS data to render the rough data processable (Glennie et al. 2013). In the study, the Terrascan, BLUH (Bundle block adjustment Leibniz University Hannover), Surfer, and LISA software were used to process the ALS data, to generate the DSM, DTM and 3D forest stand maps and to validate the accuracy of the produced models and map. In addition, the Universal Transverse Mercator 15° coordinate system and the North American Datum 1983 were utilized.

Generation of the DSM and DTM

In the related ALS data tiles, a study block which covered the study area was identified. The study block had to be wider than the study area over all the border lines to prevent erroneous edges in the DSM and DTM. Due to the lack of sufficient points in the search radius during interpolation, misleading results may be obtained from border lines. To eliminate blunders (isolated and below-ground points) from the point clouds, a three-stage filtering process (Fig. S1a in Supplementary material) was performed. First, the main top and bottom height levels of the area, according to the first and last signal echoes, were determined by drawing vertical profiles. Then, a DSM class was created, and any points that remained between the vertical profile levels were incorporated into this class. This way, any blunder points were excluded from the DSM class. Similar steps were performed to filter the DTM by only using ground points to obtain the most accurate bare topography.

Considering the nature of DSMs and DTMs, and the location geometry of ALS and TLS point clouds, different interpolation techniques were utilized in the generation of the models. During DSM generation with the ALS and TLS data, one problem was related to the presence of perpendicular objects such as trees and walls. When generating a raster DSM by considering the visible surface (top view) of the objects, several points with varying elevations were located in the same pixel due to VHR (Fig. S1b in Supplemetary material). We overcame this issue by using the maximum
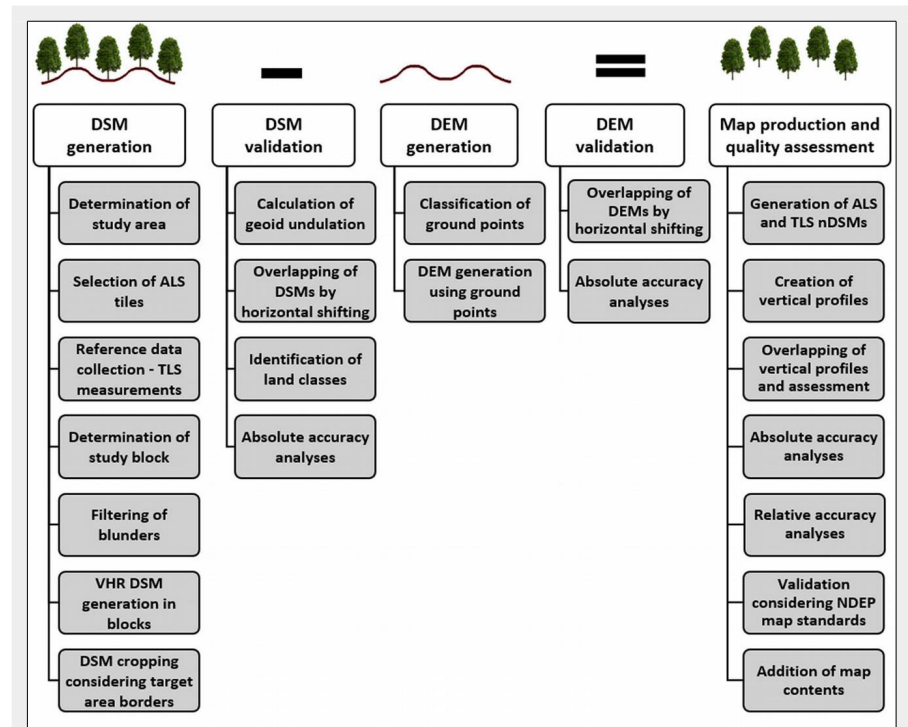
Fig. 2 - Stages of the production of a 3D forest stand height map and accuracy assessment.

point elevation within a pixel, rather than averaging, with the help of the data metrics interpolation method. In DTM generation using only ground points, the nearest neighbor interpolation method was applied. After the generation of the DSM and DTM, both the TLS and ALS models for each study block were cropped to fit the pre-determined boundaries of the study area.

Production of a 3D map of forest stand height

A 3D map of forest stand height was produced by calculating the nDSM, which is the differential calculus of a DSM and a DEM or DTM (eqn. 1):

$$nDSM = DSM - DTM$$

According to the basic principle, when bare topography is removed from the visual surface of the buildings or vegetation, what remains is the elevation of the object (Fig. S1c). In ALS, the nDSM can be summarized as the difference between the surfaces identified with the first and last backscattered echoes of the laser signal. The most significant issue in nDSM generation is the 100% horizontal overlapping of the DSM and DTM that are used. The horizontal offsets (separately in the x and y directions) between these models, which also give the horizontal geo-location accuracy of an ALS, create an insubstantial nDSM due to the calculation of wrong differentials. Due to this effect, the horizontal offsets between the generated DSM and DTM were eliminated by shifting based on an area matching cross-correlation.

Accuracy of the produced map

Accuracy assessment is one of the major processes in the production of a map created from remotely sensed data. This assessment can be performed by various techniques, which can determine the usefulness of the map according to pre-determined accuracy standards. The accuracy of 3D products generated using remotely sensed data was validated mainly by point-based comparison approaches that utilize GCPs collected by Global Navigation Satellite Systems (GNSS) measurements. However, and particularly for rough terrains, a limited number of GCPs is not adequate to assess the accuracy of 3D raster maps generated with VHR ALS point clouds, which can result in misleading numerical results and interpretations. To achieve the most reliable results, we aimed to include all the pixels of an ALS raster map in the accuracy calculation. In this context, the most eligible technique is the model-to-model comparison of the test data with reference data (Lin et al. 1994, Jacobsen 2012). When selecting the reference data, the following criteria should be fulfilled: (i) the reference data should cover the whole study area without any remarkable distortions; (ii) the resolution of the reference data has to be equal to or higher than the test data; and (iii) the absolute accuracy of the reference data should be superior to that of the test data. Considering particularly conditions (ii) and (iii), and the available mapping technologies, in the accuracy validation of a generated ALS 3D map, the TLS data was chosen as the most appropriate. The TLS point clouds were collected from four independent stations and their geo-reference

adjusted with a minimum of three external targets. The precise locations of these targets were then determined through long (> 1 hour) static surveys that used dual frequency GNSS receivers. TLS is a multi-return instrument and is therefore able to obtain measurements from all levels of the vegetation canopy, with an average point spacing of 1 cm. The dense TLS sampling and multi-return capability (sometimes > 5 returns per outgoing pulse) allowed to model the top of the canopy well with 5 mm absolute geo-location accuracy and 3 mm relative accuracy within a range of 100 m.

During the analyses, geoid undulation was applied at 27.284 m according to Geoid 12A, and the vertical geo-location accuracies were determined from the absolute standard deviation (SZ) of the height differences (eqn. 2):

$$SZ = \sqrt{\frac{\sum_{i=1}^{n} (\Delta Z_i - \mu)^2}{n-1}}$$

To estimate the effects of terrain tilt on SZ, a terrain tilt function was also calculated as follows (eqn. 3):

$$SZ_{tt} = SZ + b \cdot \tan(\alpha)$$

where SZ_{tt} is SZ expressed as function of terrain tilt, $\tan(\alpha)$ is the tangent of terrain tilt and b is a multiplicative factor.

In addition to the main indicator SZ, the root mean square error (RMSZ – eqn. 4) and the normalized median absolute elevation (NMAD) derived from median absolute deviation (MAD – eqn. 6 and eqn. 7) were used in the assessment of the absolute accuracy. In eqn. 6, i is the median of the height discrepancies between the reference and test data. SZ represents the

average, while the RMSZ is influenced by the systematic bias. The influence of systematic bias is equal to the arithmetic mean of the height differences (μ) between the reference and test data. Eqn. 5 presents the relation between the SZ and RMSZ based on bias. Due to its squared-sum nature, the SZ is strongly affected by larger discrepancies. The NMAD is based on the median, and therefore it does not change significantly if the error frequency does not correspond to a normal (symmetric) distribution. For a normal distribution, the SZ and NMAD should be almost identical (Höhle & Höhle 2009), whereas in asymmetrical cases, the error frequency description of the NMAD is superior to the SZ. Contrary to the RMSZ, it is possible to validate and identify outliers using the SZ and NMAD. In the analysis, any systematic bias that was a linear function of Z between the test and reference models was determined via linear regression, where we calculated the vertical shift and scale differences. The absolute vertical accuracies were calculated with the systematic bias eliminated (eqn. 4 to eqn. 7).

$$RMSZ = \sqrt{\frac{\sum_{i=1}^{n} \Delta Z_i^2}{n}}$$

$$RMSZ = \sqrt{SZ^2 + \mu^2}$$

$$MAD = \widetilde{x}_i |\Delta Z_i|$$

$$NMAD = 1.4815 \cdot MAD$$

The interior integrity of the produced map was determined by calculating the relative standard deviation (RSZ) based on the relationship between neighboring pixels (eqn. 8). The RSZ was estimated by separately grouping pixels and considering the distance of the current point to a reference

point for both height differences dZ [difference of Z(reference) - Z(compared point in the distance group)], when they were available (eqn. 8):

$$RSZ = \sqrt{\frac{\sum (DZ_i - DZ_j)^2}{2nx}}$$

where $D_l < D < D_u$. Hence, the height discrepancies of neighboring points were compared, and the dependency (correlation of dZ) was checked. In this way, local random errors and random errors could be separated. In the case where differences were found in the independent heights (correlation = 0), RSZ was identical to SZ, and if the correlation coefficient was 1.0, RSZ would be zero. Under normal conditions, the RSZ had a value between zero and SZ. In extreme cases of a negative correlation, the RSZ may be larger than SZ. In normal conditions, the RSZ of active remote sensing systems such as radars and lasers are superior to their absolute accuracies (Jacobsen 2003, 2012, ASPRS 2014). In eqn. 8, D represents the distance groups (the distance of the current point to a reference point, when height differences are available for both) and D_l and D_u are the lower and upper distance limits, respectively. In this study, the distance groups varied from the 1st to the 10th pixel (0.25 to 2.5 m, considering the 0.25 m pixel size of the reference TLS data), since for each pixel 10 neighboring pixels were used in the calculation. The term nx is the number of point combinations in the distance group, and n is the total number of differences between the reference and actual values. The term nx is multiplied by a factor of 2 in order to normalize RSZ to the size of SZ. If the height differences of the points in a distance group are independent, corresponding to error propagation, the RMS will be $\sqrt{2}$ times larger than SZ. This is represented by $2 \times nx$.

Results

Generated models and maps

Fig. 3 presents the DSM and DTM generated with ALS using a color scale for height. Only ground points were used in DTM generation and all non-terrain objects were eliminated. The last echo of a laser signal may not always return from the bare earth depending on the number of returns of the laser scanner. Sometimes, the last echo may return from a level of understory trees or low vegetation such as bracken or grass. This is why the point density is expected to be lower in the ground layer. As a consequence, the influence of interpolation can be seen more clearly in the DTM due to the use of further points. The solution for increasing the point density on the ground layer is to use a laser scanner which enables more returns of the signal; however, this increases the point density in all layers that results in large amounts of unnecessary data.
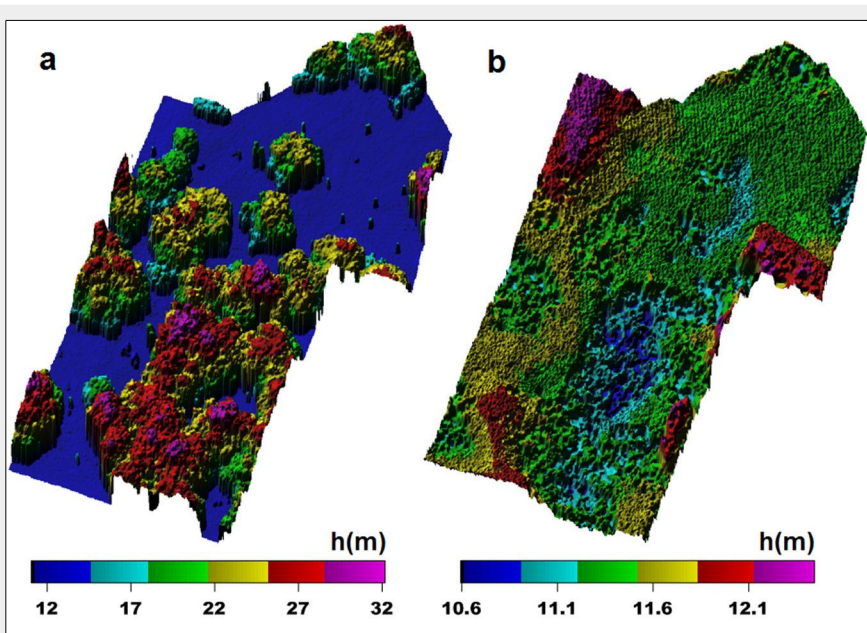
Fig. 3 - Models generated with ALS: (a) DSM; (b) DTM.

Fig. 4 - Comparison of the produced (ALS) map with the reference (TLS) map: (a) the ALS map; (b) vertical profile of the ALS map in the Y direction; (c) vertical profile of the TLS map in the Y direction; (d) comparison of the vertical profiles.
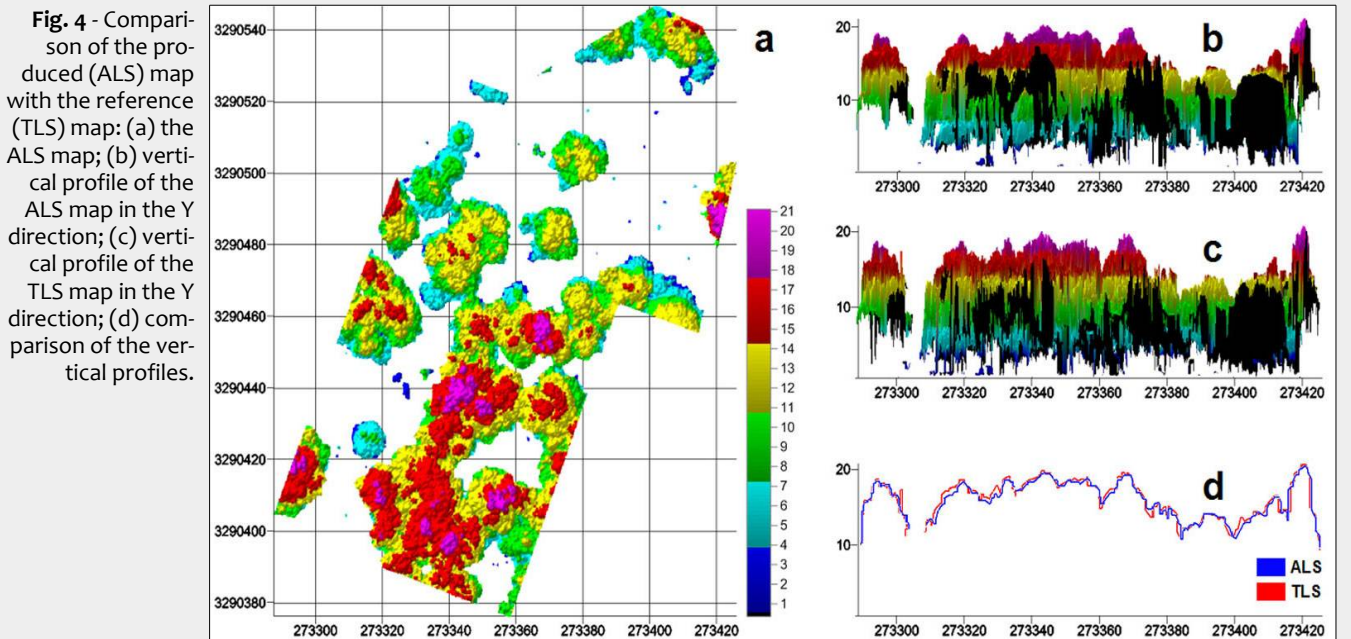
Tab. 2 - Absolute horizontal, absolute vertical accuracies and percentage of excluded points.

Reference model	Tested model	SX (cm)	SY (cm)	Bias (m)	RMSZ (m)	SZ	NMAD	SZtt	Excluded points (%)
TLS DSM (0.25m)	ALS DSM (0.25m)	0.31	-0.22	-0.48	0.498	0.149	0.071	$0.461 + 0.16 \cdot \tan(\alpha)$	10.14
				0.00	0.179	0.179	0.085	$0.109 + 0.18 \cdot \tan(\alpha)$	7.72
TLS DTM (0.25m)	ALS DTM (0.25m)	8.02	9.61	-0.23	0.270	0.135	0.134	$0.270 + 0.35 \cdot \tan(\alpha)$	0.02
				0.00	0.135	0.135	0.132	$0.182 + 0.35 \cdot \tan(\alpha)$	0.01
TLS nDSM (0.25m)	ALS nDSM (0.25m)	0.01	0.89	-0.36	0.521	0.376	0.368	$0.429 + 0.17 \cdot \tan(\alpha)$	29.94
				0.00	0.422	0.422	0.419	0.415	21.27

Fig. 4 illustrates the produced 3D map of forest stand height using a color-coded scale. For the comparison of the produced map with the reference TLS map, the vertical profiles of the ALS and TLS maps are plotted in the Y direction. It is clear that the produced map matches the reference map in almost every part of the canopy except for small disparities due to vegetation growth. In addition, the ALS map has a systematic tendency to estimate the heights of the crowns and the terrain to slightly lower values than are present in the reference TLS map. The amount of this systematic bias was determined and eliminated in the vertical accuracy assessment. In the interpretation of the data, the up-down and down-up scanning views of ALS and TLS should not be overlooked.

Accuracy of the generated models and map

Tab. 2 presents the absolute horizontal and vertical accuracies of the produced map in relation to the reference map including standard deviation of X and Y discrepancies (SX, SY), SZ, SZ as function of terrain tilt (SZtt), RMSZ and NMAD. The horizontal accuracy of the produced map is very high, and ranges from 0 to 9 cm. The vertical accuracies are given with and without the effects of systematic bias. The systematic biases varied for the DSM, DTM

and nDSM comparisons between the ALS and TLS due to using different interpolation techniques in their generation. The elimination of systematic bias was found to have a significant effect on the absolute vertical accuracy, particularly on the excluded points, which resulted in a height difference >1 m between the produced map and the reference map. The DSM and DTM assessment system, BLUH, only compared data that were available in both models, and if the test data corresponded to a gap in the reference data, this pixel was identified and excluded. As expected, in the produced map (nDSM), the vertical accuracy was lower compared to the results of the DSM and DTM due to the map only covering the forest layer and ignoring open and flat areas. In this study, the accuracy of the ALS data was evalu-

ated according to the standards developed by the American Society for Photogrammetry and Remote Sensing (ASPRS 2014) for large-scale maps based on contour interval (Tab. 3). The produced map almost fulfills the horizontal and vertical geo-location requirements for 1/2000-scaled topographic maps, which means that it can be presented at this scale.

The frequency distribution of height differences between the produced map and the reference map is shown in Fig. 5a and Fig. 5b with and without the effect of systematic bias, respectively. The height differences are normally (symmetrically) distributed for all accuracy indicators. In Fig. 5a, the SZ and NMAD clearly demonstrate the effects of bias. With the elimination of the systematic bias, all accuracy indicators are almost at the same level. Fig. 5c and

Tab. 3 - Map accuracy requirements according to map scale and contour interval (ASPRS 2014). (1): 95% confidence level (1.96×RMS).

Map scale	Contour interval (m)	Horizontal		Vertical	
		RMS (cm)	Accuracy [1] (cm)	RMS (cm)	Accuracy [1] (cm)
1:500	0.5	0.28	0.55	4.60	9.10
1:1000	1	0.56	1.10	9.25	18.2
1:2000	2	1.12	2.20	18.5	36.3
1:5000	5	2.79	5.47	46.3	90.8
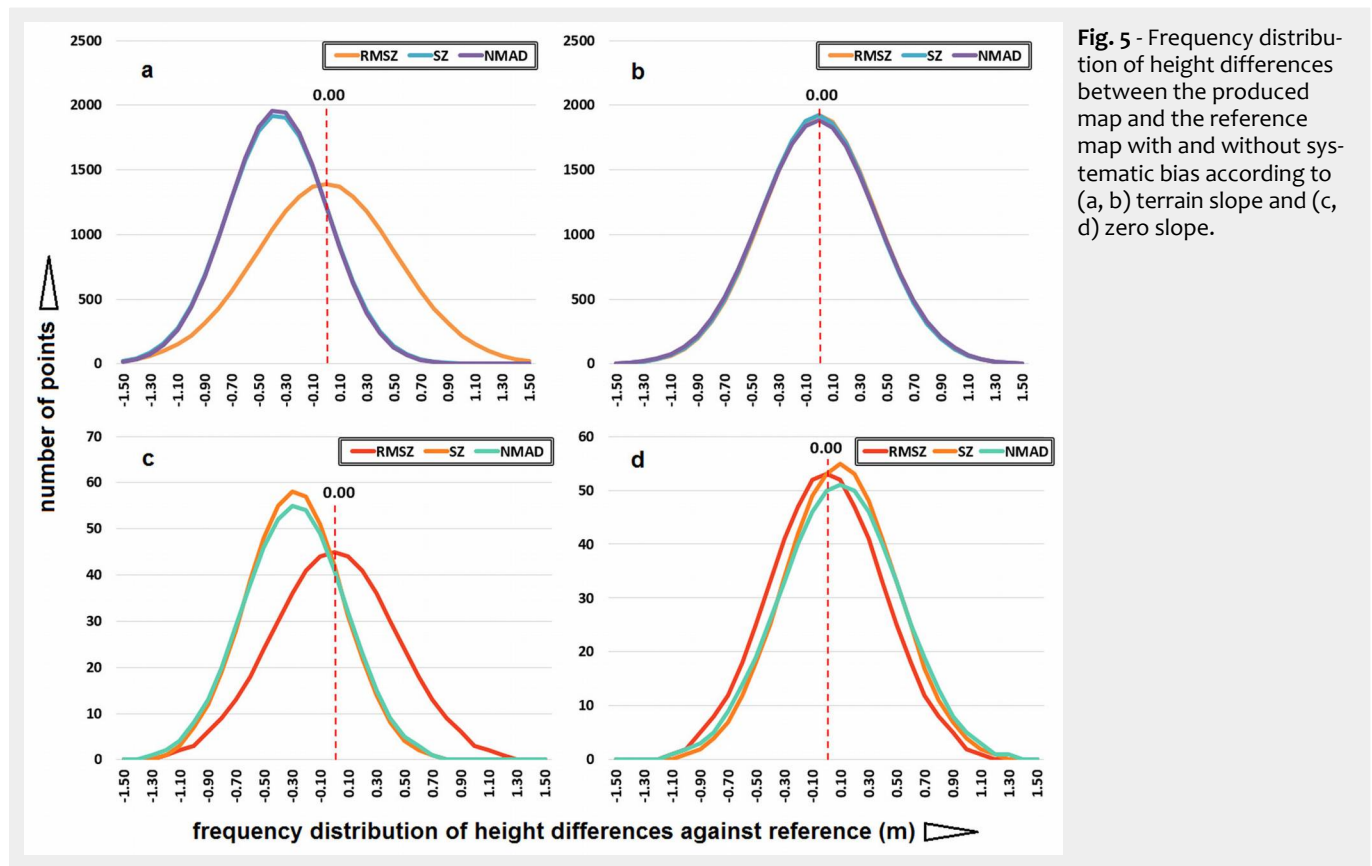
Fig. 5 - Frequency distribution of height differences between the produced map and the reference map with and without systematic bias according to (a, b) terrain slope and (c, d) zero slope.

Fig. 5d show the frequency distribution of height differences in zero slope points with and without systematic bias, respectively. A comparison of Fig. 5a and Fig. 5c gives the negative influence of terrain tilt. Without the effects of bias, the modes of all accuracy indicators are at similar levels, which are close to zero.

The accuracies of the produced map and the frequency distribution of heights are given above; however, the locations of these differences also need to be presented on the map. Therefore, a differential nDSM (Fig. 6) was generated to demonstrate the color-coded locations of differences. In the differential model, the threshold was determined as |50| cm for this product, and height differences were
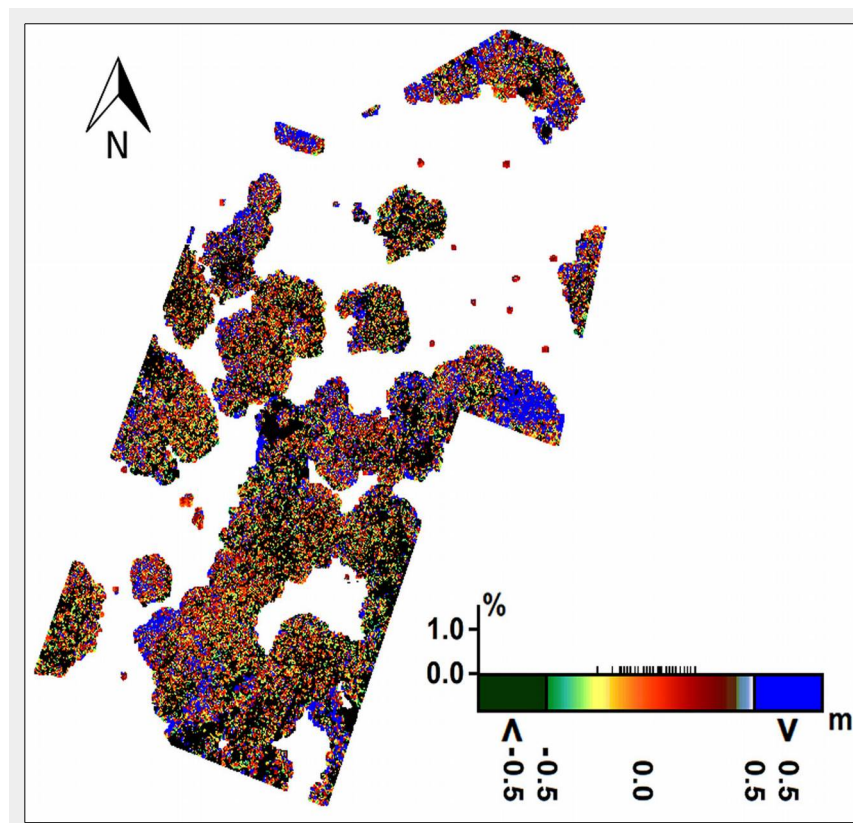
Fig. 6 - Differential nDSM including the color scale of height discrepancies (dark green = below -50 cm; blue = above 50 cm; changing colors = from -50 to +50 cm).

Tab. 4 - Relative standard deviations of produced map with and without bias.

Number of neighbored pixel	RSZ with BIAS (m)	RSZ without BIAS (m)
1	.29	.33
2	.33	.37
3	.34	.39
4	.35	.40
5	.35	.40
6	.36	.41
7	.36	.41
8	.36	.41
9	.36	.41
10	.37	.41

divided into three classes: from -50 to 50 cm; below -50 cm; and above 50 cm. Tab. 4 shows the RSZ of the produced map with and without systematic bias. As mentioned earlier, the RSZ was separately calculated for each distance group of neighboring pixels. This way, the height discrepancies of the neighboring points are compared. As shown in Tab. 4, the RSZ varies between 30 and 40 cm, and it is not larger than the SZ, which means that normal conditions apply. The analysis of the trends of RSZ with and without systematic bias indicated that there were no outliers.

Conclusions

In this study, a 3D map of forest stand height was produced using an effective remote sensing method, ALS. This method offers very high-resolution point clouds and can penetrate forest canopy through the detection of multiple echoes per each laser pulse. A suitable study area with a forest coverage of approximately 60% was selected at the University of Houston. The geo-location accuracies of the produced map were analyzed using a model-to-model, rather than a point-based, approach. The TLS data were deemed convenient as the reference data for calculations. SZ was chosen as the main accuracy indicator in addition to the use of the RMSZ and NMAD for the prediction of absolute accuracy. Furthermore, the effects of terrain tilt on the accuracy of the results were evaluated. The results demonstrate that the geo-location accuracy of the produced map is better than 1 cm horizontally and approximately 40 cm in height. According to the ASPRS standards, this accuracy is sufficient for the production of a 1/2000 scale topographic map. Another important result was about the significant effects of systematic bias on accuracy. The differences between the produced map and the reference map in terms of height frequencies were normally distributed with no outliers. The locations and the magnitudes of the height discrepancies were shown using a differential nDSM. In addition, as expected for active

remote sensing systems under normal conditions, the RSZ was superior to the absolute standard deviation.

Overall, the results clearly demonstrate that ALS data can be effectively used to produce 3D maps of forest stand height up to the 1/2000 scale.

References

Akay AE, Wing M, Sessions J (2012). Estimating structural properties of riparian forests with airborne LiDAR data. International Journal of Remote Sensing 33 (22): 7010-7023. - doi: 10.1080/01431161.2012.697206

ASPRS (2014). ASPRS positional accuracy standards for digital geospatial data. Photogrammetric Engineering and Remote Sensing 81 (3): A1-A26.

Baligh A, Valadan Zoej MJ, Mohammadzadeh A (2008). Bare earth extraction from airborne lidar data using different filtering methods. The International Archives of the Photogrammetry, Remote Sensing and Spatial Information Sciences 37 (B3b): 237-240. [online] URL: http://www.researchgate.net/publication/228821817

Baltsavias E (1999). A comparison between photogrammetry and laser scanning. ISPRS Journal of Photogrammetry and Remote Sensing 54 (2): 83-94. - doi: 10.1016/S0924-2716(99)00014-3

Glennie C, Carter WE, Shrestha RL, Dietrich WE (2013). Geodetic imaging with airborne LiDAR: the Earth's surface revealed. Reports on Progress in Physics 76 (8): 086801. - doi: 10.1088/0034-4885/76/8/086801

Hill JM, Graham LA, Henry RJ, Cotter DM, Ping A, Young P (2000). Wide-area topographic mapping and applications using airborne light detection and ranging (Lidar) technology. Photogrammetric Engineering and Remote Sensing 66 (8): 908-914. [online] URL: http://cat.inist.fr/?aModele=afficheN&cpsidt=1429409

Höhle J, Höhle M (2009). Accuracy assessment of digital elevation models by means of robust statistical methods. ISPRS Journal of Photogrammetry and Remote Sensing 64: 398-406. - doi: 10.1016/j.isprsjprs.2009.02.003

Jacobsen K (2003). DEM generation from satellite data. In: Proceedings of the "23rd EARSeL Symposium 2003: Remote Sensing in Transition" (Goossens R eds). Ghent (Belgium) 2-5 June 2003. Millpress, Rotterdam, Netherlands, pp. 513-525. [ISBN 90-5966-007-2] [online] URL: http://pdfs.semanticscholar.org/e066/f8a278f845bf2cb19c9b4e81ec4dde1e1131.pdf

Jacobsen K (2012). Characteristics of nearly world wide available digital height models. In: Proceedings of the "10th Seminar on Remote Sensing and GIS Applications in Forest Engineering". Curitiba (Brazil) 15-18 Oct 2012, pp. 8.

[online] URL: http://www.ipi.uni-hannover.de/uploads/tx_tkpublikationen/KJ_Curitiba_DEM_2012.pdf

Koch B, Heyder U, Welnacker H (2006). Detection of individual tree crowns in airborne LiDAR data. Photogrammetric Engineering and Remote Sensing 72: 357-363. - doi: 10.14358/PERS.72.4.357

Lin Q, Vesecky JF, Zebker HA (1994). Comparison of elevation derived from insar data with DEM over large relief terrain. International Journal of Remote Sensing 15 (9): 1775-1790. - doi: 10.1080/01431169408954208

Liu X (2008). Airborne LiDAR for DEM generation: some critical issues. Progress in Physical Geography 32: 31-49. - doi: 10.1177/0309133308089496

Lohr U (1998). Digital elevation models by laser scanning. The Photogrammetric Record 16 (91): 105-109. - doi: 10.1111/0031-868X.00117

Mandlburger G, Briese C, Pfeifer N (2007). Progress in LiDAR sensor technology - chance and challenge for DTM generation and data administration. In: Proceedings of the "51st Photogrammetric Week '07" (Fritz D ed). Wichmann Verlag, Heidelberg, Germany, pp. 159-169.

McIntosh K, Krupnik A, Schenk A (2000). Improvement of automatic DSM generation over urban areas using airborne laser scanner data. International Archives of Photogrammetry and Remote Sensing 33 (B3): 563-570. [online] URL: http://www.isprs.org/proceedings/XXXIII/congress/part3/563_XXXIII-part3.pdf

Shan J, Sampath A (2005). Urban DEM generation from raw lidar data: a labeling algorithm and its performance. Photogrammetric Engineering and Remote Sensing 71 (2): 217-226. - doi: 10.14358/PERS.71.2.217

Smreček R (2012). Utilization of ALS data for forestry purposes. In: Proceedings of the "6th GI Forum 2012: Geovizualisation, Society and Learning" (Jekel T, Car A, Strobl J, Griesebner G eds). Salzburg (Austria) 2-6 July 2012. H. Wichmann Verlag, VDE Verlag GMBH, Berlin, Offenbach, Germany, pp. 365-375. [online] URL: http://www.researchgate.net/publication/265040386

Sterenczak K, Bedkowski K, Weinacker H (2008). Accuracy of crown segmentation and estimation of selected trees and forest stand parameters in order to resolution of used DSM and nDSM models generated from dense small footprint LIDAR data. International Archives of Photogrammetry and Remote Sensing 37 (B6b): 27-32. [online] URL: http://citeseerx.ist.psu.edu/viewdoc/download?doi=10.1.1.184.3620&rep=rep1&type=pdf

Supplementary Material

Fig. S1 - (a) Filtering of blunders, (b) elevation variety trouble in same pixel, (c) nDSM basic principle.

Link: Sefercik_2039@suppl001.pdf